

Rare strange particle decays

M. Zamkovsky

on behalf of the NA62 Collaboration
Charles University, Prague, Czech Republic

The rare decays $K^+ \rightarrow \pi^+ \nu \bar{\nu}$ and $K_L \rightarrow \pi^0 \nu \bar{\nu}$ are extremely attractive processes to study flavor physics because they are both exceptionally clean from a theoretical point of view. These modes are measured by the experiments NA62 at CERN in Switzerland and KOTO at J-PARC in Japan, respectively. The latest results from these experiments together with future prospects are presented. The NA62 experiment has, besides the main goal, a rich physics program on other rare kaon decays which will be also discussed.

I. INTRODUCTION

Kaon physics is still in the main scope of both theoretical and experimental physics. The ultra rare kaon decays $K^+ \rightarrow \pi^+ \nu \bar{\nu}$ and $K_L \rightarrow \pi^0 \nu \bar{\nu}$ are particularly of interest. They have very precise theoretical prediction that makes them sensitive to physics beyond the Standard Model (SM). So far only the charged mode has been observed by the experiments E787 and E949 at Brookhaven National Laboratory [1]. The result obtained with a kaon decay-at-rest technique is: $BR(K^+ \rightarrow \pi^+ \nu \bar{\nu}) = (17.3_{-10.5}^{+11.5}) \times 10^{-11}$, consistent with the SM expectation within its large statistical uncertainty. The neutral mode has an upper limit at 90% CL $BR(K_L \rightarrow \pi^0 \nu \bar{\nu}) < 2.6 \times 10^{-8}$ set by the E391a experiment [2]. The NA62 experiment aims to measure the branching ratio of the $K^+ \rightarrow \pi^+ \nu \bar{\nu}$ decay with an error comparable to the theoretical prediction and the KOTO experiment wants to make an observation of the neutral mode.

The NA62 experimental apparatus can measure a variety of other processes besides the main goal. Specifically, the further physical program includes search for Heavy Neutral Leptons (HNL), Lepton Flavour and Lepton Number Violation (LFV and LNV), searches for dark photons, inflatons, etc.

II. PHYSICS MOTIVATION

The $K^+ \rightarrow \pi^+ \nu \bar{\nu}$ and $K_L \rightarrow \pi^0 \nu \bar{\nu}$ modes are flavor changing neutral current (FCNC) decays that are theoretically exceptionally clean. They proceed through box and electroweak penguin diagrams and, thanks to a quadratic GIM mechanism and a strong Cabibbo suppression, are extremely rare. Using the value of tree-level elements of the Cabibbo-Kobayashi-Maskawa (CKM) matrix as external inputs, the SM predicts [3, 4]:

$$\begin{aligned} BR(K^+ \rightarrow \pi^+ \nu \bar{\nu}) &= (8.4 \pm 1.0) \cdot 10^{-11}, \\ BR(K_L \rightarrow \pi^0 \nu \bar{\nu}) &= (3.4 \pm 0.6) \cdot 10^{-11}. \end{aligned} \quad (1)$$

The theoretical origin of these processes is dominated by short distance contribution without hadronic

uncertainties as the hadronic matrix elements are extracted from the well-known decay $K^+ \rightarrow \pi^0 e^+ \nu$. As the perturbative QCD and electroweak corrections in both decays are under full control, the theoretical error budget within the SM is dominated by the CKM parameter uncertainties.

The $K \rightarrow \pi \nu \bar{\nu}$ decays are extremely sensitive to physics beyond the SM, probing the highest mass scales among the rare meson decays. Large deviations are expected in several beyond the SM scenarios [5]. For example, the tree-level FCNC mediated by heavy gauge boson (Z') [6], should show a specific correlations between $BR(K^+ \rightarrow \pi^+ \nu \bar{\nu})$ and $BR(K_L \rightarrow \pi^0 \nu \bar{\nu})$. In the recent models with Lepton Flavour Universality violation [7], the anomalies observed in the semileptonic B meson decays could be linked to $BR(K^+ \rightarrow \pi^+ \nu \bar{\nu})$ measurement.

III. EXPERIMENTAL SETUP

A. NA62

The NA62 experiment uses the protons from the CERN SPS accelerator, which impinge on a beryllium target and produce a secondary hadron beam at nominal momentum of 75 GeV/c and 1% momentum spread (rms) at 750 MHz, about 6% of which are kaons. The beam is accompanied by a muon halo at the nominal rate of 3 MHz in the detector acceptance. The first upstream detectors are the Differential Cerenkov counter (KTAG) used to identify K^+ in the beam, the silicon pixel beam spectrometer GTK and the Charged Anti-counter detector, used to suppress products of inelastic interactions in the GTK. They are followed by a 110 m long vacuum tank defining the fiducial volume (FV) in first 60 m, where about 13% of the K^+ entering the experiment decay. It contains the four tracking stations of the magnetic spectrometer. Around the vacuum tube twelve ring-shaped Large Angle Vetoes (LAV) are located with increasing diameter with distance from the target, which together with the electromagnetic Liquid Krypton calorimeter (LKr), the Inner Ring Calorimeter (IRC) and Small Angle Calorime-

ter (SAC) provide hermetic acceptance for photons emitted in the K^+ decays for polar angle up to 50 mrad. A Ring-Imaging Cherenkov counter (RICH) for particle identification and two plastic scintillator charged hodoscopes (CHOD) are located downstream of the vacuum tank, before the LKr. For further particle identification two hadronic calorimeters and muon veto detector (MUV1,2,3) follow the LKr. Additional counters (MUV0, HASC) installed at optimized locations provide hermetic coverage for charged particles produced in multi-track kaon decays. The schematic layout of the detector is shown in Fig. 1 and the full detector description can be found in [8].

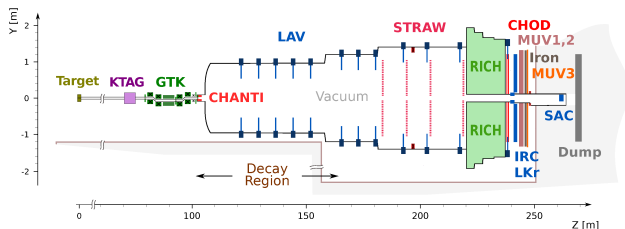


FIG. 1. Schematic side view of the NA62 experiment.

B. KOTO

The KOTO experiment [12] at J-PARC is a fixed target detector using primary protons at 30 GeV/c extracted from the J-PARC Main Ring accelerator and directed onto a 66 mm-long gold target. The secondary K_L beam, accompanied with neutrons and photons, with a peak momentum of 1.4 GeV/c is produced at an angle of 16 degrees with respect to the nominal beam. A halo of neutrons produced in the collimators, traveling outside of the nominal beam solid angle, are present. The decay volume is a 3 m long chamber evacuated down to 5×10^{-7} mbar to suppress π^0 produced in the interactions of beam neutrons with the residual gas. The signature of $K_L \rightarrow \pi^0 \nu \bar{\nu}$ are two photons from π^0 and nothing else, so the main signal detector is an electromagnetic calorimeter CSI. It consist of 2716 undoped CsI crystals, 50 cm long and $2.5 \times 2.5 (5 \times 5)$ cm² cross section within (outside) the central 1.2×1.2 m² region, with a hole in the middle to let the beam particles pass through. The veto counters outside of the decay region consist of lead-scintillator sandwich, lead-aerogel, or undoped-CsI counters for photons and plastic scintillators or wire chambers for charged particles. After the 2013 Physics run, KOTO implemented several improvements to the experimental apparatus. These include: reduced thickness of the vacuum window from 125 μ m to 12 μ m; added beam profile monitor for better beam alignment; added beam pipe charged veto. The detailed description of the experimental setup can

be found in [9, 10] and the schematic layout is in Fig. 2.

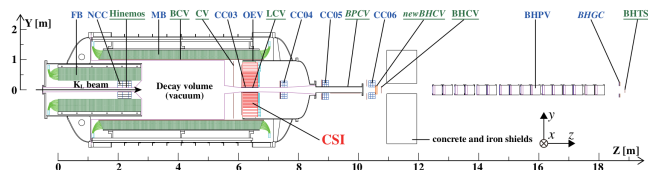


FIG. 2. Layout of the KOTO experiment. Detector components with their abbreviated names written in blue (in green and underlined) are photon (charged particle) veto counters.

IV. THE NA62 $K^+ \rightarrow \pi^+ \nu \bar{\nu}$ ANALYSIS

The signature of the signal is one charged track in GTK compatible with a kaon hypothesis and one in the detector downstream. Kaon decays and beam-related activity are sources of background. During the 2016 data taking, a sample of $N_K = 1.1(2) \times 10^{11}$ was collected and further analyzed.

A. Event Selection

The squared missing mass calculated from an upstream K^+ 4-momentum p_K and a downstream π^+ 4-momentum p_π ($m_{miss}^2 = (p_K - p_\pi)^2$) is used to discriminate kinematically the main K^+ decay modes from the signal. Based on m_{miss}^2 spectrum, two signal regions on either side of the $K^+ \rightarrow \pi^+ \pi^0$ peak are defined (see Fig. 3). The signal events must have a π^+ momentum in the (15,35) GeV/c range. The distribution of m_{miss}^2 as a function of the π^+ momentum from a control data sample is depicted in Fig. 4. Kinematic selection is not powerful enough to separate signal from background events, so the additional suppression by π^+ identification (ID), photon and multiplicity rejection is required. The particle identification is based on the RICH measurement and a multivariate analysis of calorimetric information from LKr, MUV1 and MUV2, with MUV3 information used as veto. The π^+ ID efficiency within (15,35) GeV/c momentum range is 78% (82%) using calorimeters (RICH), and the corresponding muon mis-ID as π^+ is 0.6×10^{-5} (2.1×10^{-3}), respectively.

Photon rejection requires no in-time activity in any of the LAV, IRC, SAC and no additional clusters in the LKr beyond 100 mm radius around the π^+ impact point. Multiplicity rejection criteria against photons interacting in the detector material upstream of the LKr include: no in-time activity in the hodoscopes unrelated to the π^+ but in spatial coincidence with an energy deposit of at least 40 MeV in the LKr; no additional segments reconstructed in the STRAW compat-

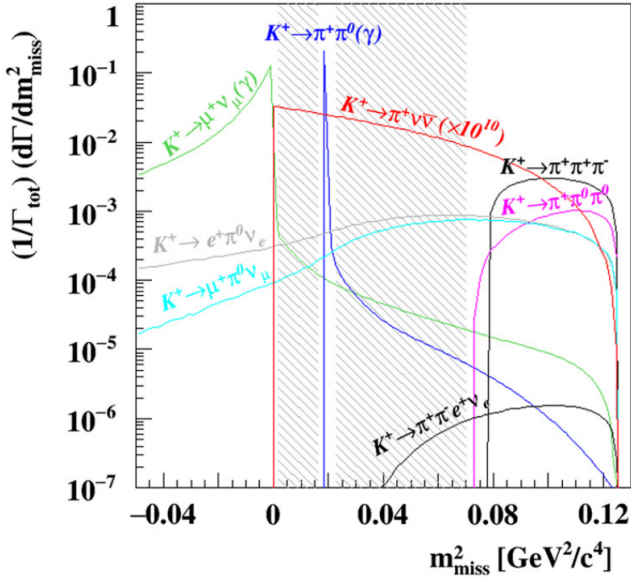


FIG. 3. True m_{miss}^2 distribution of the $K^+ \rightarrow \pi^+ \nu \bar{\nu}$ decay together with the main K^+ decay modes, computed under π^+ mass hypothesis in the final state. The signal (red) is multiplied by a factor of 10^{10} for a better visibility, and dashed areas show the signal regions.

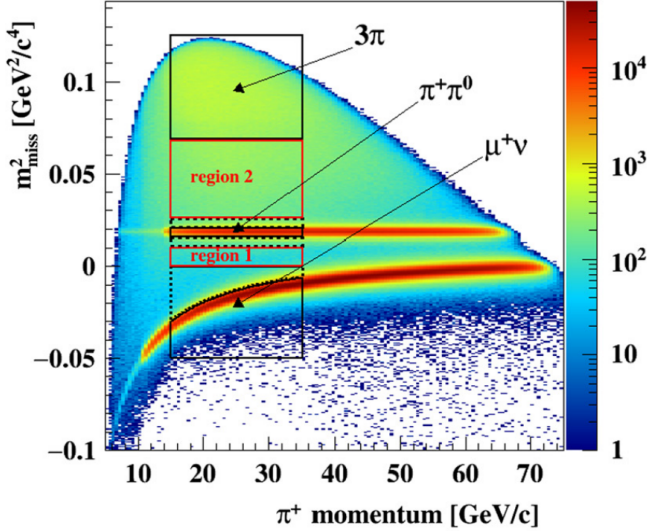


FIG. 4. Distribution of the m_{miss}^2 as a function of the π^+ momentum based on a control data sample. The main backgrounds together with the signal regions are highlighted.

ible with the decay vertex; no in-time signals in HASC and MUV0; fewer than four extra signals in the hodoscope in time with the π^+ . The resulting $\pi^0 \rightarrow \gamma\gamma$ rejection inefficiency is measured to be 2.5×10^{-8} at 10% (24%) signal loss due to π^+ interactions (accidentals). Photon and multiplicity rejection is also effective against $K^+ \rightarrow \pi^+ \pi^+ \pi^-$ and $K^+ \rightarrow \pi^+ \pi^- e^+ \nu$

backgrounds.

B. Single Event Sensitivity

The single event sensitivity is defined as $SES = 1/(N_K \cdot \varepsilon_{\pi\nu\nu})$, where N_K is the number of K^+ decays in the fiducial volume and $\varepsilon_{\pi\nu\nu}$ is the signal efficiency, taking into account the selection acceptance, trigger efficiency and photon plus multiplicity rejection inefficiency. The particle identification inefficiency is included in the selection acceptance $A_{\pi\nu\nu} = (4.0 \pm 0.1)\%$, which is evaluated using MC simulation. The number of kaons was obtained from the normalization mode $K^+ \rightarrow \pi^+ \pi^0$ selected in the same way as the signal except for photon and multiplicity rejection and requiring m_{miss}^2 to be in the $\pi^+ \pi^0$ region.

The SES and the corresponding number of SM $K^+ \rightarrow \pi^+ \nu \bar{\nu}$ decays expected in the signal regions are:

$$SES = (3.15 \pm 0.01_{stat} \pm 0.24_{syst}) \times 10^{-10}, \quad (2)$$

$$N_{\pi\nu\nu}^{exp}(SM) = 0.267 \pm 0.001_{stat} \pm 0.020_{syst} \pm 0.032_{ext}.$$

The systematic uncertainty includes those of $A_{\pi\nu\nu}$, trigger efficiency, photon and multiplicity rejection inefficiency. The external error refers to uncertainties of the SM parameters.

C. Expected Background and Results

Background from K^+ decays in the FV is mainly due to $K^+ \rightarrow \pi^+ \pi^0(\gamma)$, $K^+ \rightarrow \mu^+ \nu(\gamma)$, $K^+ \rightarrow \pi^+ \pi^+ \pi^-$ and $K^+ \rightarrow \pi^+ \pi^- e^+ \nu$ decays. Other kaon decays give negligible contribution, estimated at $\mathcal{O}(10^{-3})$. The upstream backgrounds are due to pions originating upstream of the fiducial volume. They are produced in: K^+ decays between GTK stations 2 and 3, matching an accidental beam particle; elastic scattering of beam π^+ in GTK 2 and 3, matched to an accidental K^+ ; K^+ interactions with beam line material, produced either promptly or as a decay product of a neutral kaon.

The table I gives a summary of all background sources.

After unmasking the signal regions, one event is found in Region 2, as shown in Fig. 5.

Considering the observation of one event, the p -value of the signal and background hypothesis is 15% and the corresponding observed upper limit is:

$$BR(K^+ \rightarrow \pi^+ \nu \bar{\nu}) < 14 \times 10^{-10} \text{ at } 95\% \text{ CL}. \quad (3)$$

A detailed description of the analysis procedure and background estimation can be found in [11].

TABLE I. Summary of the background estimates summed over the two signal regions.

Process	Expected events in R1+R2
$K^+ \rightarrow \pi^+ \pi^0(\gamma)$ IB	$0.064 \pm 0.007_{stat} \pm 0.006_{syst}$
$K^+ \rightarrow \mu^+ \nu(\gamma)$ IB	$0.020 \pm 0.003_{stat} \pm 0.006_{syst}$
$K^+ \rightarrow \pi^+ \pi^- e^+ \nu$	$0.013^{+0.017}_{-0.012} _{stat} \pm 0.009_{syst}$
$K^+ \rightarrow \pi^+ \pi^+ \pi^-$	$0.002 \pm 0.001_{stat} \pm 0.002_{syst}$
$K^+ \rightarrow \pi^0 \mu^+ \nu, K^+ \rightarrow \pi^0 \mu^+ \nu$	< 0.001
$K^+ \rightarrow \pi^+ \gamma \gamma$	< 0.002
Upstream background	$0.050^{+0.090}_{-0.030} _{stat}$
Total Background	$0.152^{+0.092}_{-0.033} _{stat} \pm 0.013_{syst}$

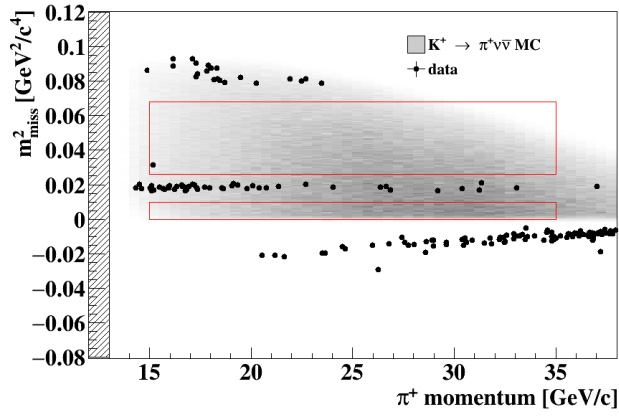


FIG. 5. Reconstructed m_{miss}^2 as a function of momentum of π^+ (markers) satisfying the $K^+ \rightarrow \pi^+ \nu \bar{\nu}$ selection, except the m_{miss}^2 and π^+ momentum criteria. The grey area corresponds to the expected distribution of $K^+ \rightarrow \pi^+ \nu \bar{\nu}$ MC events. Red contours define the signal regions.

D. Future Prospects

The 2016 result is based on 2% of the total NA62 exposure in 2016/2018 and demonstrates the validity of the decay-in-flight technique in terms of background rejection and in view of the measurement in progress using the full data sample. The analysis of 2017 data sample is ongoing with the 2016-like event selection, hence has a comparable analysis performance. However, there are some improvements in the treatment of the pileup in IRC and SAC resulting in 40% lower π^0 rejection inefficiency and slightly improved usage of RICH variables. The 2017 data set also allows the detailed comparison between signal and background shapes in the signal regions as a function of π^+ momentum. The preliminary estimations are summarized in table II.

TABLE II. Preliminary estimation of expected SM $K^+ \rightarrow \pi^+ \nu \bar{\nu}$ events and background contributions based on 2017 data sample.

PRELIMINARY	
N_K	$(13 \pm 1) \times 10^{11}$
SES	$(0.34 \pm 0.04) \times 10^{-10}$
$K^+ \rightarrow \pi^+ \nu \bar{\nu}$	2.5 ± 0.4
Background	
$K^+ \rightarrow \pi^+ \pi^0(\gamma)$ IB	$0.35 \pm 0.02_{stat} \pm 0.03_{syst}$
$K^+ \rightarrow \mu^+ \nu(\gamma)$ IB	$0.16 \pm 0.01_{stat} \pm 0.05_{syst}$
$K^+ \rightarrow \pi^+ \pi^- e^+ \nu$	$0.22 \pm 0.08_{stat}$
$K^+ \rightarrow \pi^+ \pi^+ \pi^-$	$0.015 \pm 0.008_{stat} \pm 0.015_{syst}$
$K^+ \rightarrow \pi^+ \gamma \gamma$	$0.005 \pm 0.005_{syst}$
$K^+ \rightarrow \ell^+ \pi^0 \nu_\ell$	$0.012 \pm 0.012_{syst}$
Upstream background	Analysis on-going

V. THE KOTO $K_L \rightarrow \pi^0 \nu \bar{\nu}$ ANALYSIS

The KOTO experiment collected $N(K_L) \sim 2.4 \times 10^{11}$ and reached single event sensitivity at the level of ($SES 1.3 \times 10^{-8}$) in 2013. An upper limit on $BR(K_L \rightarrow \pi^0 \nu \bar{\nu})$ was set to $< 5.1 \times 10^{-8}$ at 90% CL [10].

During 2015 a data set of 2.2×10^{19} protons on target was collected. The event selection is based on the π^0 reconstruction of from two clusters above 3 MeV in CSI. The π^0 decay vertex Z_{vtx} and transverse momentum P_t were calculated assuming that the vertex was on the beam axis. The Z_{vtx} for signal candidates was required to lie in the range $3000 < Z_{vtx} < 4700$ mm to avoid π^0 's generated by halo neutrons hitting detector components. The requirement on P_t as a function of Z_{vtx} greatly suppresses the background from $K_L \rightarrow \pi^+ \pi^- \pi^0$ decays. To reduce a class of $K_L \rightarrow \pi^0 \pi^0$ decays with miscombination of two photons in the π^0 reconstruction, a requirement on the photons energies ratio and the product of their energy and the angle between the beam axis and their momenta is imposed. The opening angle cut in the transverse plane was required to reduce the $K_L \rightarrow \gamma \gamma$ background, in which the photons are back to back. To select π^0 candidates with plausible kinematics, allowed regions were set on $(P_t/P_z, Z_{vtx})$ and (E, Z_{vtx}) planes, where P_z and E are the longitudinal momentum and energy of the π^0 , respectively. This cut was effective also to reduce the background from η mesons produced in the halo-neutron interaction with the of plastic scintillator veto-counter for charged particles (CV) [12] located in front of CSI. Other neutron-induced backgrounds are upstream π^0 and ‘‘hadron cluster’’, caused by neutron directly hitting CSI and creating a hadronic shower and by a neutron produced in the primary shower to create a second, separated hadronic shower. Table III gives

a summary of the different background contributions.

TABLE III. Summary of background estimation.

source	Expected events in signal region
K _L decay	
K _L → π ⁺ π ⁻ π ⁰	0.05 ± 0.02
K _L → π ⁰ π ⁰	0.02 ± 0.02
Other K _L decays	0.03 ± 0.01
Neutron induced	
Hadron cluster	0.24 ± 0.17
Upstream-π ⁰	0.04 ± 0.03
CV-η	0.04 ± 0.02
Total	0.42 ± 0.18

After full event selection no signal candidate events were observed, as shown in Fig. 6. Assuming Poisson statistics with uncertainties taken into account, the upper limit on BR(K_L → π⁰νν̄) < 3.0 × 10⁻⁹ at 90% CL was obtained [13], improving the upper limit of the direct search by almost an order of magnitude.

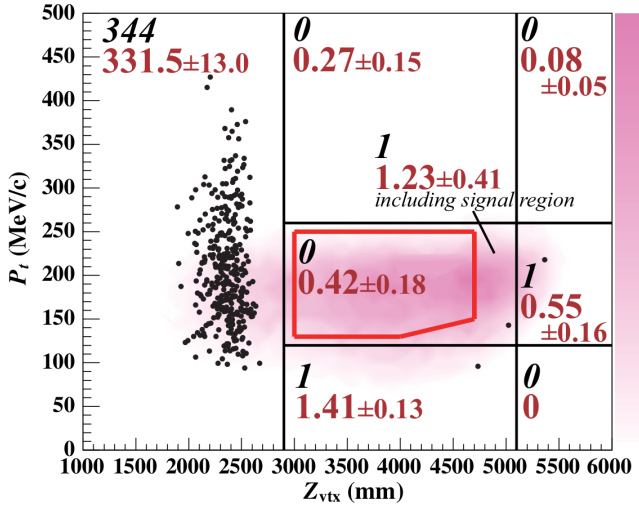


FIG. 6. Reconstructed π⁰ transverse momentum (P_t) as a function of its decay vertex position Z_{vtx} . The region surrounded by red lines is the signal region. Black markers represent observed events, and the contour indicates the K_L → π⁰νν̄ signal distribution derived from the MC simulation. The black (red) numbers represent observed (expected background) events for the regions inside the lines.

The data collected in years 2016-2018 are under study and the results are expected soon, in the summer of 2019. The preliminary estimates look very promising, with $SES = 8.2 \times 10^{-10}$ and total background of 0.20 ± 0.16 .

VI. OTHER KAON DECAY STUDIES AT NA62

A search for LFV/LNV in three track kaon decays was performed on data taken during three months in 2017, which corresponds to about 30% of the data collected in 2016-2018. The forbidden decays K⁺ → π⁻μ⁺μ⁺ and K⁺ → π⁻e⁺e⁺ were analyzed. All the details of the analysis can be found in [14]. The upper limits at 90% CL are BR(K⁺ → π⁻e⁺e⁺) < 2.2 × 10⁻¹⁰ and BR(K⁺ → π⁻μ⁺μ⁺) < 4.2 × 10⁻¹¹. They are improving the current PDG limits [15] by a factor of three in electron mode and by a factor of two in muon mode.

A search for HNL was completed on the 2015 data set and is published in [16]. Upper limits on the HNL mixing parameters $|U_{\ell 4}|^2$ at 90% CL were established in the ranges 170-448 MeV/c² and 250-373 MeV/c² for positron and muon modes, respectively, at a level between 10⁻⁷ and 10⁻⁶, see Fig. 7. Major improvements are foreseen with the new data taken in years 2016-2018.

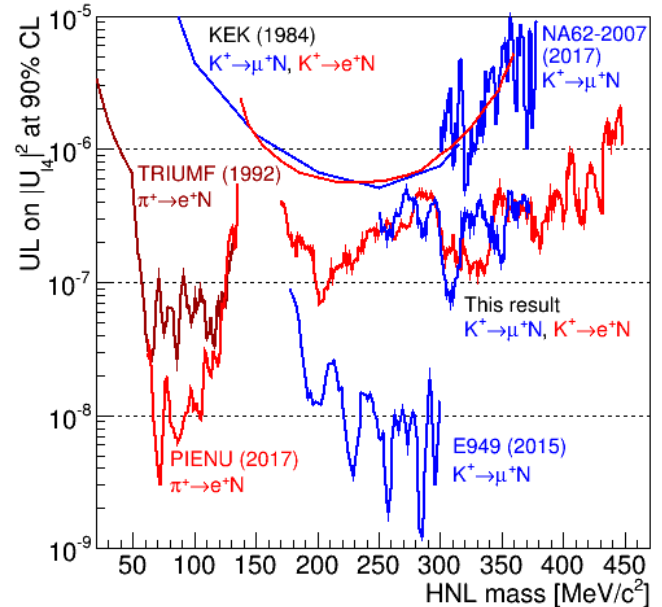


FIG. 7. Upper limits on $|U_{\ell 4}|^2$ at 90% CL obtained for each assumed HNL mass compared to other experimental results.

VII. CONCLUSION

The latest results on flavor physics golden modes K⁺ → π⁺νν̄ and K_L → π⁰νν̄ are reported.

The charged mode is measured by the NA62 experiment to set the upper limits BR(K⁺ → π⁺νν̄) < 14 × 10⁻¹⁰ at 95% CL [11]. A major improvement is

foreseen when the already collected data will be fully analyzed.

The KOTO experiment measured the neutral mode on 2013 and 2015 data sets. The upper limit on $\text{BR}(\text{K}_L \rightarrow \pi^0 \nu \bar{\nu})$ was obtained to be $< 5.1 \times 10^{-8}$ at 90% CL based on 2013 data [10], and $\text{BR}(\text{K}_L \rightarrow \pi^0 \nu \bar{\nu}) < 3.0 \times 10^{-9}$ at 90% CL from 2015 data set [13].

The results on HNL and LFV/LNV studies by the NA62 experiment are also discussed. For LFV/LNV modes, the upper limits at 90% CL are $\text{BR}(\text{K}^+ \rightarrow \pi^- e^+ e^+) < 2.2 \times 10^{-10}$ and $\text{BR}(\text{K}^+ \rightarrow \pi^- \mu^+ \mu^+) < 4.2 \times 10^{-11}$ [14]. For HNL upper limits

are set on the HNL mixing parameters $|U_{\ell_4}|^2$ at 90% CL [16].

ACKNOWLEDGMENTS

Support for this work has been received from the grant LTT 17018 of the Ministry of Education, Youth and Sports of the Czech Republic and from Charles University Research Center UNCE/SCI/013.

-
- [1] A. V. Artamonov *et al.* [BNL-E949 Collaboration], *Phys. Rev. D* **79**, 092004 (2009).
 - [2] J. K. Ahn *et al.* [E391a Collaboration], *Phys. Rev. D* **81**, 072004 (2010).
 - [3] J. Brod, M. Gorbahn and E. Stamou, *Phys. Rev. D* **83**, 034030 (2011).
 - [4] A. J. Buras, D. Buttazzo, J. Girrbach-Noe and R. Knegjens, *JHEP* **1511**, 033 (2015).
 - [5] M. Blanke, A. J. Buras and S. Recksiegel, *Eur. Phys. J. C* **76**, 182 (2016).
 - [6] A. J. Buras, D. Buttazzo and R. Knegjens, *JHEP* **1511**, 166 (2015).
 - [7] M. Bordone, D. Buttazzo, G. Isidori and J. Monnard, *Eur. Phys. J. C* **77**, 618 (2017).
 - [8] E. Cortina Gil *et al.* [NA62 Collaboration], *JINST* **12**, P05025 (2017).
 - [9] T. Yamanaka [KOTO Collaboration], *PTEP* **2012**, 02B006 (2012).
 - [10] J. K. Ahn *et al.* [KOTO Collaboration], *PTEP* **2017**, 021C01 (2017).
 - [11] E. Cortina Gil *et al.* [NA62 Collaboration], *Phys. Lett. B* **791**, 156 (2019).
 - [12] D. Naito *et al.*, *PTEP* **2016**, 023C01 (2016).
 - [13] J. K. Ahn *et al.* [KOTO Collaboration], *Phys. Rev. Lett.* **122**, 021802 (2019).
 - [14] E. Cortina Gil *et al.* [NA62 Collaboration], arXiv:1905.07770.
 - [15] M. Tanabashi *et al.* (Particle Data Group), *Phys. Rev. D* **98**, 030001 (2018).
 - [16] E. Cortina Gil *et al.* [NA62 Collaboration], *Phys. Lett. B* **778**, 137 (2018).